Non-Born–Oppenheimer variational calculations of HT+ bound states with zero angular momentum

Eugeniusz Bednarz
Department of Chemistry, University of Arizona, Tucson, Arizona 85721

Sergiy Bubin
Department of Physics, University of Arizona, Tucson, Arizona 85721 and Department of Chemistry, University of Arizona, Tucson, Arizona 85721

Ludwik Adamowicz
Department of Chemistry, University of Arizona, Tucson, Arizona 85721 and Department of Physics, University of Arizona, Tucson, Arizona 85721

We report fully nonadiabatic calculations of all rotationless bound states of HT+ molecular ion $(t^+p^+e^-)$ carried out in the framework of the variational method. We show that, in all the states, except the two highest ones, the bond in the system can be described as covalent. In the highest two states the bond becomes essentially ionic and HT+ can be described as a T+H+ complex. The wave function of the system was expanded in terms of spherically symmetric, explicitly correlated Gaussian functions with preexponential multipliers consisting of powers of the internuclear distance. Apart from the total energies of the states, we have calculated the expectation values of the *t-p*, *t-e*, and *p-e* interparticle distances, their squares, and the nucleus-nucleus correlation functions. © *2005 American Institute of Physics*. [DOI: 10.1063/1.1884602]

I. INTRODUCTION

The HD+ molecular ion has been a model system for studies of the nonadiabatic coupling between the electronic and nuclear motions. The lack of a center of symmetry in this system due to different nuclear masses requires that the theoretical approach for calculating its stationary bound states is somewhat different than that applied to the parent symmetric cation, H_2^+, where an obvious placement of the center of the internal coordinate system is the middle of the bond. Since the HT+ has even larger nuclear mass difference than HD+, the approach applied to both systems may be similar. While the asymmetry of the HD+ system has been extensively investigated both experimentally[1–3] and theoretically,[4–6] including our recent work,[7] there have been only a few studies (only theoretical) concerning the HT+ molecular ion.[8–10]

In a recent work Ben-Itzhak *et al.*[2] studied the dissociation of the electronic ground state of HD+ following ionization of HD by fast proton impact and discovered that the H++D(1*s*) dissociation channel is more likely than the H(1*s*)+D+ channel by about 7%. This symmetry breakdown can only be explained if the finite nuclear mass correction to the Born–Oppenheimer (BO) approximation is taken into account. In our non-BO calculation,[7] we showed that while in the first 21 vibrational states $(v=1,2,\ldots,20)$ only minor charge asymmetry is present in the wave functions, in the highest two states $(v=21$ and $v=22)$ HD+ is strongly polarized and the system can be described as a complex of D and H+ (D+H+ is also the lowest energy dissociation product of the HD+ ion).

In this work we consider the charge asymmetry of the HT+ ion. Due to a larger mass difference between the nuclei in HT+ than in HD+, one could expect a stronger charge polarization and a larger number of the vibrational states near the dissociation threshold with the "ionic" character. However, the results of this work will show that this appears not to be the case. Apart from describing the charge asymmetry in HT+, another goal of this work has been to provide high accuracy estimates of the nonrelativistic energies for all rotationless vibrational states of this ion, which have not been calculated before, except for few low lying ones.[9,10]

If the starting point of considering the HT+ ion is its representation based on the BO approximation, the charge asymmetry in the system appears as a nonadiabatic coupling between the *gerade* and *ungerade* electronic states. The two states mix due to the coupling of the nuclear and electronic motions. The coupling increases near the dissociation limit where the dissociation energy becomes comparable to the total energy difference of H and T atom ground states.

The T atom is energetically more stable than H because it has slightly larger reduced mass, which makes the average electron-nucleus distance slightly shorter in T than in H resulting in stronger coulombic attraction and lower energy. Thus, upon dissociation, HT+ splits into T+H+ which is a lower-energy dissociation product than T++H. There are two previous theoretical works concerning HT+ that need to be mentioned. Bishop[8] and Bishop and Cheung[9] first applied an approach to HT+ that did not involve the adiabatic approximation and was based on the variational principle. They calculated the ground and the first two excited vibrational states, as well as a few lowest rotational states of the ion. Most recently, Frolov[10] applied a fully nonadiabatic variational approach using exponential basis function with complex parameters to refine the total ground-state energies for

the heteronuclear and homonuclear isotopomers of H_2^+, including HT^+. In this work we compare our energy results with those of Bishop and Cheung, and of Frolov.

In the present work, we use the approach we have developed to perform rigorous ground-state and excited state non-BO calculations on diatomic systems with an arbitrary number of electrons.[11–19] The approach is based on separating the operator describing the center of mass kinetic energy from the total Hamiltonian of the system and representing the remaining internal Hamiltonian in the reference frame centered at one of the particles (in most cases the heaviest particle). In the calculation we use the explicitly correlated n-particle Gaussian functions to expand the spatial part of the wave function. No approximation is made in the approach apart from neglecting the relativistic effects and using a finite basis set expansion of the wave function. As we have demonstrated on a number of cases, including, for example, the H_2 molecule,[15] and most recently the HD^+ ion,[7] the approach produces very accurate results.

Since the vibrational quantum number is not a "good" quantum number in the non-BO calculation (only the values of the square of the total, i.e., electronic plus nuclear, angular momentum and its projection on a selected axis are good quantum numbers) we need to explain what we mean by the term "vibrational spectrum." Our use of the term refers to the ground and excited states with certain value of the total angular momentum. In the present calculations this has been the ground rotational state (i.e., the state with zero total angular momentum; the rotationless state).

In this work, we have also calculated the expectation values of all interparticle distances (i.e., r_{p-t}, r_{p-e}, and r_{t-e}) and their squares for all considered states. The algorithm for calculating those quantities is shown in the Appendix. The comparison of the $\langle r_{p-e} \rangle$ and $\langle r_{t-e} \rangle$ has allowed us to examine the charge asymmetry that occurs in HT^+. To our knowledge, this is the first direct calculation of these quantities for this system that uses rigorous nonadiabatic wave functions.

Although the present calculations have concerned the whole rotationless HT^+ spectrum, our main focus was the highest few vibrational states where the most significant charge asymmetry is expected to occur. Thus, while all the states have been calculated with very high precision, in the highest two states the number of basis function was significantly increased to improve the precision even further. Not only this generated better energy values for those states, but also allowed to examine the convergence of the procedure in terms of the number of the basis functions in the wave function expansion. Since the wave functions of the highest two states contain the largest number of radial nodes, these states were the most difficult to describe. The analysis of the convergence of the energy and the averaged interparticle distances performed for the two states show how reliable the calculations are not only for those states, but also for the other states where, due to fewer radial nodes, the basis set size did not have to be as large.

II. THE HAMILTONIAN

In the approach we use,[11] we begin with the total nonrelativistic Hamiltonian for a molecular system in the laboratory Cartesian coordinates. All particles present in the system are included in the Hamiltonian. For HT^+ it looks as follows (in atomic units):

$$\hat{H}_{TOT} = -\sum_{i=1}^{3} \frac{1}{2M_i} \nabla_{\mathbf{R}_i}^2 + \sum_{i=1}^{3} \sum_{j>i}^{3} \frac{Q_i Q_j}{R_{ij}}, \tag{1}$$

where M_i's, Q_i's, and positions $\mathbf{R}_i$'s are the masses, the charges, and the position vectors of the tritium nucleus, the proton, and the electron respectively ($M_1=m_t$, $M_2=m_p$, $M_3=m_e$, $Q_1=1$, $Q_2=1$, $Q_3=-1$), and where $R_{ij}=|\mathbf{R}_j-\mathbf{R}_i|$ are interparticle distances. Note that no distinction between the electron and the nuclei is made and the two types of particles are treated equivalently. In the next step, we transform the laboratory coordinate system to a new coordinate system, whose first three coordinates are the Cartesian coordinates describing the position of the center of mass in the laboratory coordinate system and the remaining six coordinates are internal coordinates. The internal coordinates are defined with respect to a Cartesian coordinate system whose origin is placed at the tritium nucleus and whose axes are parallel to the axes of the laboratory coordinate frame. The first three of the six internal coordinates, $\mathbf{r}_1=|\mathbf{R}_2-\mathbf{R}_1|$, describe the position of the proton with respect to the coordinate origin and the last three, $\mathbf{r}_2=|\mathbf{R}_3-\mathbf{R}_1|$, describe the position of the electron. Using the new coordinates, we can separate the Hamiltonian representing the motion of the center of mass in the laboratory coordinate system from the internal Hamiltonian, $\hat{H}_{INT}=\hat{H}$, thereby reducing the three-particle problem to a two-pseudoparticle problem. The internal Hamiltonian has the following form:

$$\hat{H} = -\frac{1}{2}\left(\sum_{i=1}^{2} \frac{1}{m_i} \nabla_{\mathbf{r}_i}^2 + \sum_{i \neq j}^{2} \frac{1}{M_1} \nabla'_{\mathbf{r}_i} \nabla_{\mathbf{r}_j}\right) + \sum_{i=1}^{2} \frac{q_0 q_i}{r_i} + \sum_{i<j}^{2} \frac{q_i q_j}{r_{ij}}. \tag{2}$$

This Hamiltonian describes a system containing the reference particle (triton) at the origin of the coordinates with charge $q_0=Q_1=1$ and two pseudoparticles, or internal particles, with reduced masses $m_1=m_t m_p/(m_t+m_p)$ and $m_2=m_t m_e/(m_t+m_e)$, and charges $q_1=1$ and $q_2=-1$. Thus, the wave function describing the internal motion of the system, $\Psi(\mathbf{r}_1,\mathbf{r}_2)$, is dependent on the Cartesian coordinates of two pseudoparticles, the first resembling the proton and the second resembling the electron. The second term in the parenthesis in Eq. (2) is the mass polarization term, which arises from the coordinate transformation and which couples the motion of the two pseudoparticles. In the potential energy term, r_i and r_{ij} are defined as $r_i=|\mathbf{r}_i|=|\mathbf{R}_{i+1}-\mathbf{R}_1|$ and $r_{ij}=|\mathbf{R}_{j+1}-\mathbf{R}_{i+1}|=|\mathbf{r}_j-\mathbf{r}_i|$.

Since the mass of the pseudoproton is much larger than the mass of the pseudoelectron, all lower bound states of the system correspond to excitations (either "rotational" or "vibrational") of the nuclear motion. In particular, as mentioned before, if the calculation is restricted only to rotationless states (i.e., fully spherically symmetric states), only the vibrational states are obtained. In those states, higher excitation should generate larger numbers of radial nodes in the wave function in terms of the pseudoproton coordinates.

Another important feature of the eigenfunctions of the Hamiltonian (2), which does not appear in the electronic states, results from the repulsion of the pseudoproton with the positive charge at the coordinate origin. Due to the repulsion, the wave function should significantly decrease in magnitude when the distance of the pseudoproton to the origin shortens. For bound states the wave function should also become smaller for larger distances. In between, the vibrational wave function should reach a maximum (near the equilibrium internuclear distance for the considered state) and, depending on the excitation level, it should have several radial oscillations. The basis set used in the calculation should be capable of describing these features very accurately.

III. THE WAVE FUNCTION

In our previous works, we have shown that the explicitly correlated Gaussian basis set involving, functions with pre-exponential multipliers consisting of the internuclear distance $\mathbf{r}_1$ raised to a non-negative even power m_k (Refs. 12 and 13)

$$\phi_k = r_1^{m_k}\exp[-\mathbf{r}'(A_k \otimes I_3)\mathbf{r}] \tag{3}$$

is capable of very effectively describing nonadiabatic zero angular momentum states of diatomic systems with σ electrons. In those functions, the combination of the preexponential powers of the internuclear distance and the Gaussian exponents dependent on the coordinates of all pseudoparticles and their relative distances describes very effectively the correlated motion of the pseudonucleus and the pseudoelectrons in the central potential of the positive charge located at the origin of the coordinate system. The exponential coefficients in the Gaussian (3) form the symmetric matrix A_k. In our calculations, this matrix is expressed as a product of an $n \times n$ lower triangular matrix L_k of rank n and its transpose, L_kL_k'. This is done to avoid dealing with constraints that would need to be imposed on the elements of the matrix A_k due to the required square itegrability of functions (3) in the optimizations of the A_k matrix elements. With the use of the L_kL_k' decomposition of A_k, the square itegrability is automatically satisfied for any variation of the elements of L_k in the range $[-\infty, \infty]$. In Eq. (3), I_3 is the 3×3 identity matrix, and in general, I_n is the $n \times n$ identity matrix, $\otimes$ denotes the Kronecker Product, and $\mathbf{r}$ is a $3n \times 1$ vector of the internal Cartesian coordinates $\mathbf{r}_i$ of the n pseudoparticles. The fact that functions (3) correspond to zero total angular momentum follows from their rotational invariance.[11]

In the HT⁺ calculations, the spin free wave functions, $\Psi(\mathbf{r}) = \Psi(\mathbf{r}_1, \mathbf{r}_2)$, for all rotationless states have been generated as expansions in terms of two-particle Gaussians of the form given by the expression (3):

$$\Psi(\mathbf{r}) = \sum_{k=1}^{K} c_k \phi_k(\mathbf{r}). \tag{4}$$

The powers m_k ranged from 0 to 250 in the calculations. This rather extended range of powers was needed to accurately represent oscillations of the vibrational part of the wave functions which are particularly strong in highly excited states.

IV. THE VARIATIONAL CALCULATIONS

The ground-state and excited state nonadiabatic wave functions for HT⁺ in the present calculations were obtained by minimizing the Rayleigh quotient:

$$E(\{c_k\}, \{m_k\}, \{L_k\}) = \min_{\{\{c_k\}, \{m_k\}, \{L_k\}\}} \frac{c'H(\{m_k\}, \{L_k\})c}{c'S(\{m_k\}, \{L_k\})c} \tag{5}$$

with respect to the basis function exponential parameters $\{L_k\}$ and the preexponential powers $\{m_k\}$. The minimum with respect to the expansion coefficients of the wave function in terms of the basis functions c_k was found by solving the secular equation.

Much of the recent progress in the area of very accurate non-BO diatomic calculations has been due to the derivation and implementation of analytical gradients of the energy functional (5) with respect to variational nonlinear parameters of the basis functions. In the minimization of the energy functional, the availability of the analytical gradient of the energy leads to significant acceleration of the optimization process and allows one to apply the procedure to functionals dependent on hundreds or even thousands of variational parameters.

To achieve the best results in the parameter optimization with the least computational effort, we have recently implemented a hybrid approach that combines the gradient based optimization with the stochastic selection method.[16,17] The strategy is based on alternating the gradient based and the stochastic based optimizations in growing the basis set from a small initial set generated in a gradient based optimization to the final set. The basis set for each vibrational state was generated in a separate calculation. To reach high accuracy in the calculations, we used a 1500-term expansion for the ground and first excited states, a 2000-term expansions for $v = 2, 3$ states, a 2500-term expansions for $v = 4$–17 states, a 3000-term expansion for $v = 18$–20 states, a 4000-term expansion for $v = 21$ state. In the calculations for the two highest excited states ($v = 22, 23$), where the charge symmetry breaking is the most significant, we increased the length of the expansion to 5000. Having the energy determined with several basis set expansion lengths for the highest two states allowed analysis of the convergence of the procedure in terms of the number of basis functions. The calculations have been carried out at the University of Arizona Center of Computing and Information Technology with the use of an HP Alpha GS1280 supercomputer.

After the wave functions for all 24 ($v = 0, \ldots, 23$) states were generated, we calculated the expectation values of the internuclear triton–proton distance, $\langle r_{t\text{-}p} \rangle$, the triton–electron ($t$-$e$) distance, $\langle r_{t\text{-}e} \rangle$, and the proton–electron (p-e) distance, $\langle r_{p\text{-}e} \rangle$, for each state. We also calculated the average values of the squares of the distances. The derivation of the formula for calculating the expectation values is given in the Appendix. In our calculations, we used the following values for the nuclear masses: $m_t = 5496.921\,503m_e$, where m_e stands for

TABLE I. Total energies, expectation values of the triton-proton distance, r_{t-p}, the triton-electron distance, r_{t-e}, and the proton-electron distance, r_{p-e}, and their squares for the rotationless bound states of HT$^+$. All quantities are in atomic units. K is the number of basis functions.

v	K	E	$\langle r_{t-p} \rangle$	$\langle r_{t-e} \rangle$	$\langle r_{p-e} \rangle$	$\langle r^2_{t-p} \rangle$	$\langle r^2_{t-e} \rangle$	$\langle r^2_{p-e} \rangle$	E, other works
0	1500	−0.598 176 134 5	2.051	1.686	1.687	4.252	3.525	3.528	−0.598 176 134 4, Ref. 9[a]
									−0.598 176 134 669 766 232, Ref. 10[b]
1	1500	−0.589 932 813 7	2.161	1.744	1.745	4.802	3.811	3.816	−0.589 932 813 1, Ref. 9[a]
2	2000	−0.582 080 048 6	2.274	1.804	1.805	5.397	4.120	4.125	−0.582 080 024 8, Ref. 9[a]
3	2000	−0.574 606 743 5	2.391	1.866	1.867	6.041	4.452	4.458	
4	2500	−0.567 503 159 8	2.513	1.930	1.932	6.741	4.811	4.818	
5	2500	−0.560 760 877 7	2.639	1.997	1.999	7.502	5.200	5.209	
6	2500	−0.554 372 772 0	2.771	2.067	2.069	8.333	5.625	5.635	
7	2500	−0.548 333 001 5	2.910	2.140	2.143	9.244	6.090	6.103	
8	2500	−0.542 637 011 4	3.056	2.217	2.220	10.25	6.602	6.618	
9	2500	−0.537 281 546 4	3.211	2.299	2.302	11.36	7.169	7.189	
10	2500	−0.532 264 693 1	3.377	2.386	2.390	12.61	7.803	7.828	
11	2500	−0.527 585 922 4	3.556	2.479	2.484	14.01	8.516	8.549	
12	2500	−0.523 246 148 0	3.750	2.580	2.587	15.60	9.328	9.372	
13	2500	−0.519 247 835 9	3.963	2.690	2.699	17.43	10.26	10.32	
14	2500	−0.515 595 121 7	4.199	2.813	2.825	19.58	11.35	11.43	
15	2500	−0.512 293 913 8	4.467	2.950	2.966	22.12	12.65	12.77	
16	2500	−0.509 352 167 1	4.775	3.106	3.130	25.23	14.22	14.39	
17	2500	−0.506 779 939 2	5.138	3.288	3.324	29.12	16.17	16.45	
18	3000	−0.504 589 807 9	5.582	3.505	3.564	34.20	18.68	19.18	
19	3000	−0.502 796 855 1	6.149	3.771	3.879	41.22	22.05	23.03	
20	3000	−0.501 419 014 9	6.925	4.097	4.345	51.82	26.74	29.19	
21	4000	−0.500 476 391 2	8.139	4.412	5.259	70.67	32.85	42.28	
22	5000	−0.499 998 389 3	11.11	3.068	9.590	129.6	21.63	113.0	
23	5000	−0.499 917 007 3	19.91	1.729	19.72	424.4	5.706	424.2	
T[c]		−0.499 909 056 5		1.500			3.001		

[a]Obtained with the following mass ratios: $m_e/m_p = 0.000\ 544\ 617$, $m_e/m_t = 0.000\ 181\ 920$.
[b]Obtained with $m_p = 1836.152\ 701 m_e$, $m_t = 5496.921\ 58 m_e$.
[c]T atom in the ground state.

the mass of the electron $m_p = 1836.152\ 672\ 61 m_e$. These values were taken from CODATA 2002 (Ref. 20) list of fundamental constants.

V. RESULTS AND DISCUSSION

In Table I we compare our variational energy values for the $v = 0-23$ states of HT$^+$ with the energy values of some states available in the literature. In the same table we also show the expectation values of the interparticle distances and their squares obtained in the calculations. As one could expect, the average internuclear distance increases with the rising level of excitation. This increase becomes more pronounced as the excitation level approaches the dissociation threshold. For $v = 21$, $v = 22$, and $v = 23$ states (the highest levels corresponding to a bound state) the average internuclear distance increases from 8.139 a.u. to 11.11 a.u., and then to 19.91 a.u. respectively. In the $v = 23$ state, the HT$^+$ ion is only bound by 8×10^{-6} hartree and the system is almost dissociated.

Our HD$^+$ calculations demonstrated[7] that system becomes essentially ionic in the last two rotationless vibrational states. As the results in Table I show, the same effect occurs in the HT$^+$ ion, though the charge asymmetry in the highest state is somewhat lower than that in the highest state of HD$^+$. In this highest state of HT$^+$ the t-e average distance is 1.729 a.u., while the p-e distance is 19.72 a.u. Due to this

high asymmetry the HT$^+$ bond in this state can be described as ionic. In the lower states, as it was the case with the HD$^+$ ion, some charge asymmetry is also present in the t-e and p-e distances and this asymmetry progressively increases with the increasing excitation level. However, the HT$^+$ bond in the $v = 0-21$ states can still be described as mostly covalent.

To illustrate the convergence of the energy and the expectation values of the interparticle distances, we show in Table II the results for the ground ($v = 0$) and for the highest two states ($v = 22$ and 23) obtained with different basis sizes ranging from 500 to 5000. The two highest states are the most difficult to describe due to the highest number of radial nodes in their wave functions and due to their significant spacial diffuseness. The results presented in Table II show that both the energy and the distances converged quite well. With 1500 functions in the basis for the ground state, the energy is converged in nine significant figures. For the highest states the number of converged figures is 8. One may expect that to reach a similar convergence level for all states one needs to progressively increase the number of basis functions going from the bottom to the top of the spectrum. This is what has been done in the present calculations as shown by the number of functions used for each state shown in the second column in Table I. However, as the Gaussians are usually less effective in describing the electronic and nuclear cusps than the other regions of the wave function, there may be some residual error left in our energies. Our

TABLE II. The convergence of the energy and the expectation values of the interparticle distances for the $v=22$ and 23 states with the number of the basis functions. All quantities in atomic units.

Basis size	E	$\langle r_{t\text{-}p}\rangle$	$\langle r_{t\text{-}e}\rangle$	$\langle r_{p\text{-}e}\rangle$	$\langle r_{t\text{-}p}^2\rangle$	$\langle r_{t\text{-}e}^2\rangle$	$\langle r_{p\text{-}e}^2\rangle$
$v=0$							
500	−0.598 176 131 581	2.051 46	1.685 83	1.686 77	4.251 88	3.524 75	3.528 36
1000	−0.598 176 134 461	2.051 46	1.685 83	1.686 77	4.251 88	3.524 75	3.528 36
1500	−0.598 176 134 523	2.051 46	1.685 83	1.686 77	4.251 88	3.524 75	3.528 36
$v=22$							
1500	−0.499 998 284 200	11.112 0	3.065 97	9.592 28	129.596	21.613 9	112.997
2000	−0.499 998 357 753	11.112 3	3.066 93	9.591 62	129.617	21.625 5	113.006
2500	−0.499 998 374 833	11.111 9	3.067 22	9.590 90	129.607	21.628 8	112.993
3000	−0.499 998 382 517	11.111 7	3.067 36	9.590 52	129.602	21.630 4	112.986
3500	−0.499 998 386 283	11.111 7	3.067 39	9.590 48	129.602	21.630 8	112.986
4000	−0.499 998 387 919	11.111 6	3.067 42	9.590 41	129.601	21.631 2	112.985
4500	−0.499 998 388 479	11.111 6	3.067 43	9.590 38	129.601	21.631 3	112.984
5000	−0.499 998 389 388	11.111 6	3.067 52	9.590 29	129.601	21.632 6	112.983
$v=23$							
1500	−0.499 916 942 558	19.860 2	1.727 55	19.671 8	420.994	5.683 77	420.804
2000	−0.499 916 992 542	19.917 4	1.728 51	19.728 1	424.495	5.700 50	424.289
2500	−0.499 917 000 467	19.913 8	1.728 76	19.724 2	424.349	5.703 90	424.139
3000	−0.499 917 003 246	19.915 3	1.728 80	19.725 7	424.486	5.704 30	424.276
3500	−0.499 917 004 628	19.914 5	1.728 84	19.724 9	424.451	5.704 91	424.240
4000	−0.499 917 005 576	19.913 9	1.728 89	19.724 2	424.423	5.705 46	424.212
4500	−0.499 917 006 555	19.913 4	1.728 90	19.723 7	424.402	5.705 66	424.191
5000	−0.499 917 007 306	19.913 0	1.728 93	19.723 2	424.383	5.705 96	424.171

estimation for that error in the $v=22$ state of HD⁺ with 4000 terms in the basis was about 10^{-9} hartree (see Table II in Ref. 7). An error of the same order of magnitude is probably also present in our 5000–term energy results for the $v=22$ and 23 states of HT⁺.

The lower effectiveness of Gaussians in describing the cusps is also likely to be partially responsible for the difference between our ground state energy and the value recently reported by Frolov,[10] who used complex exponential basis functions, and shown in Table I. In order for our ground-state energy to become closer to Frolov's result, we would need to increase the precision of real numbers in our calculations from double (15 digits) to quadruple. This would make the optimization less affected by the numerical noise and more effective. There is another source of the discrepancy between Frolov's ground-state energy and ours. It is due to the difference in the proton and triton masses (we used the most current ones, which are slightly lighter leading to our ground-state energy being slightly higher than Frolov's). In order to test how much of a difference this would make, we recalculated the energies of all states using the masses given in Frolov's paper and we found that our result for the ground-state shifts down by about 4×10^{-11} hartree. The shift increases with the excitation level and reaches a maximum for the states in the middle of the spectrum ($v=11-13$) where it becomes approximately equal to 4×10^{-10} hartree. For the highest levels the shift again becomes smaller, by an order of magnitude. This behavior is expected as it is known that the nonadiabatic effects are the most significant in the middle of the vibrational spectrum.

In our recent work[21] we developed an algorithm to calculate and plot the pseudonucleus density (or, as it can be also called, the nucleus-nucleus correlation function) based on the wave function obtained in the non-BO calculation. The pseudonucleus density is defined as

$$g(\boldsymbol{\xi}) = \langle\Psi(\mathbf{r})|\delta(\mathbf{r}_1 - \boldsymbol{\xi})|\Psi(\mathbf{r})\rangle = \int |\Psi(\boldsymbol{\xi},\mathbf{r}_2)|^2 d\mathbf{r}_2. \quad (6)$$

The algorithm has been applied in this work to show the pseudoproton density for different states of the HT⁺ ion. In Figs. 1 and 2 we show the pseudoproton densities in the two-dimensional (2D) and 3D forms for a few states from the bottom, middle, and the top of the spectrum. We included both 2D and 3D plots because, while the former better show the radial behavior of the pseudonucleus density, the latter better demonstrate the spherical radial symmetry of this quantity. In the highest, $v=23$, state the wave function and, thus, the density have 23 radial nodes. Judging from the energy values, the Gaussian basis set we use is capable of describing this very complicated nodal structure very well. One might be somewhat surprised by the fact that in Fig. 1 for the $v=23$ state the curve does not touch the ξ axis before the last oscillation (see the enlarged fragment of the plot).

Our interpretation of this effect is the following. In the non-Born–Oppenheimer calculation the wave function describes simultaneous motion of nuclei and electrons (or, as should be more correctly described, the motion of pseudonuclei and pseudoelectrons). Obviously, the wave function for the highest state has to be orthogonal to the wave functions of all lower states. For rotationless states this orthogonality can be achieved by the wave function for the highest state having the highest number of radial nodes. As mentioned before, the radial nodes can appear in the wave function for HT⁺ in terms of the pseudoproton coordinate r_1 but one can-
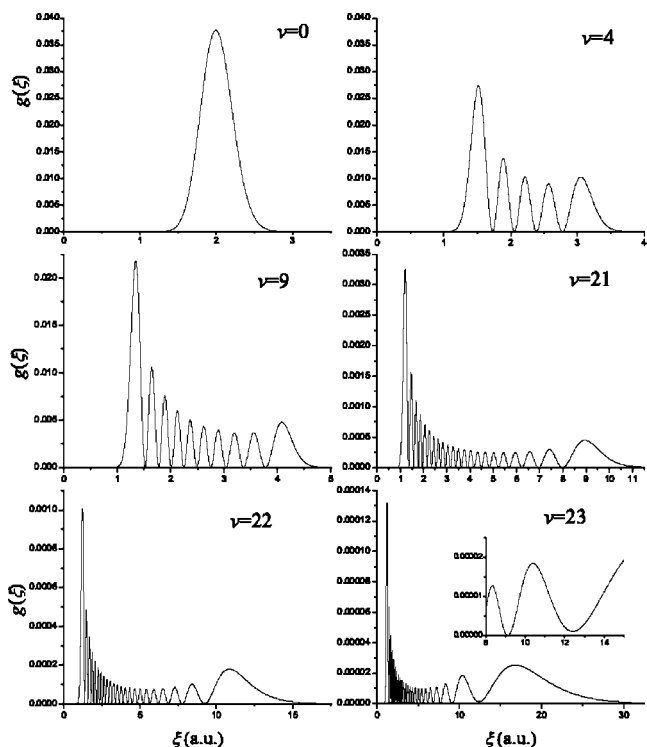
FIG. 1. Correlation functions for the ground state and for the 4, 9, 21, 22, and 23 excited states of HT$^+$.

not exclude a possibility that, especially for the highest states, there may be a component in the wave function with a node in the pseudoelectron coordinate r_2. If this is the case the density for the $v=23$ state will be a sum of two contri-

butions, one with 23 nodes in terms of r_1 and the second one with a node in terms of r_2 and fewer nodes (or even no nodes) in terms of r_1. This is a possible explanation of why we see some upshift of the density function away from the ξ axis at the last node for the $v=23$ state. If this explanation is correct, the effect is purely nonadiabatic beause it results from mixing of two electronic states.

VI. SUMMARY

In this work, rigorous, variational, high accuracy, nonadiabatic calculations employing explicitly correlated Gaussian basis functions have been performed for the HT$^+$ ion to determine its complete vibrational spectrum corresponding to zero rotational quantum number. This is the first work reporting non-BO energies for all the vibrational states of this system. The wave functions obtained in the calculations were used to determine expectation values of the t-p, t-e, and p-e distances. Those values showed that, while the bond in HT$^+$ in the lowest 22 vibrational states can be described as covalent, in the highest two states it becomes ionic. In those states the ion becomes a complex of T$+p$. In $v=23$ state the electron becomes entirely localized around the tritium nucleus and almost completely absent at the proton. This strong, purely nonadiabatic effect occurs when the dissociation energy of a vibrationally excited state becomes close to the difference between the total energies of the H and T atoms.
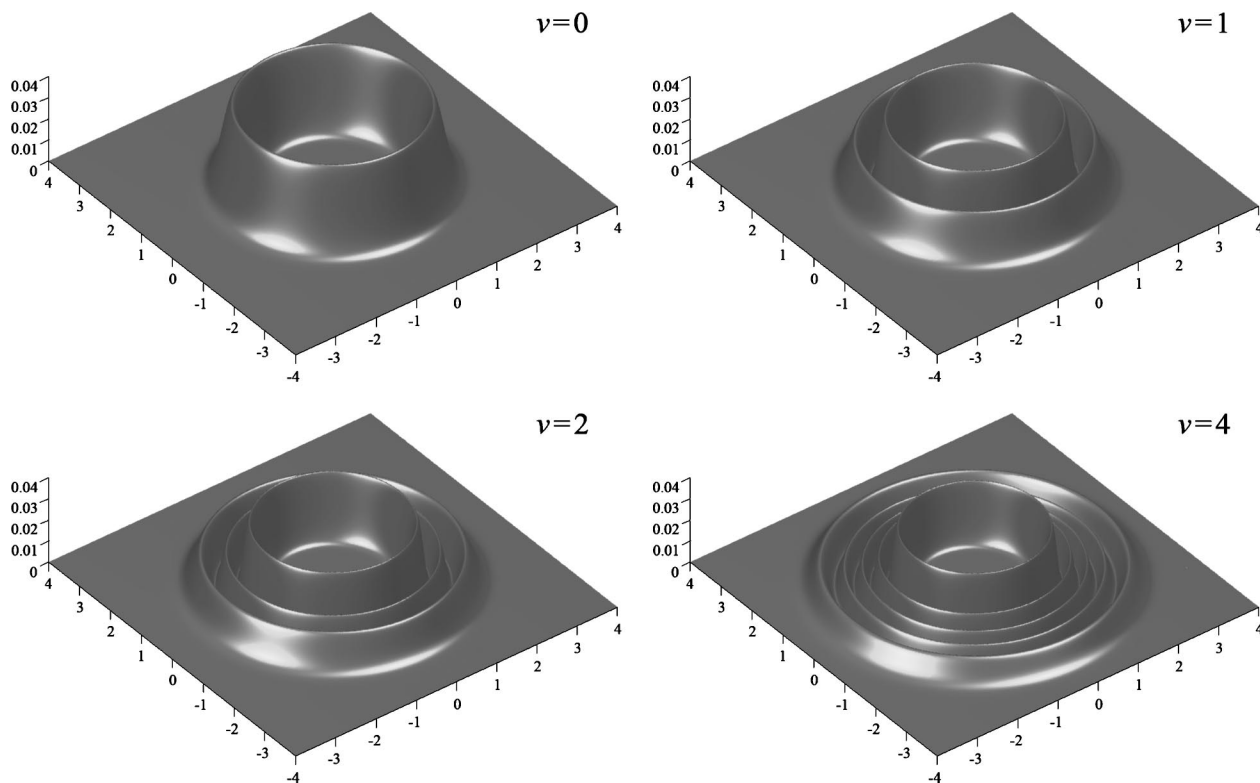

FIG. 2. 3D plots of the correlation functions, $g(\xi_x, \xi_x, \xi_z=0)$, for the ground state and for the first, second, and fourth excited states of HT$^+$. ξ_x and ξ_y (x and y axis, respectively) are in a.u.

ACKNOWLEDGMENTS

APPENDIX: STRUCTURAL INTEGRALS

First, let us recall some definitions and theorems concerning matrix properties, which we will use in the derivation of the distance matrix elements.

The Taylor expansion has the form

$$f(x) = \sum_{i=0}^{\infty} \frac{f^{(n)}(x_0)}{n!}(x - x_0)^n. \qquad (A1)$$

The Pochhammer symbol is defined as

$$(a)_n = \prod_{k=0}^{n-1}(a+k) = \frac{\Gamma[a+n]}{\Gamma[a]}, \qquad (A2)$$

where $(a)_0 = 1$, and $\Gamma[x]$ is the Euler gamma function.

We will use the Leibniz formula to determine the Nth derivative of the product of functions f and g:

$$(f \circ g)^{(N)} = \sum_{k=0}^{N}\binom{N}{k}f^{(N-k)}g^{(k)}. \qquad (A3)$$

Also, we will use a rank one J_{ij} matrix, which is defined as

$$J_{ij} = \begin{cases} E_{ii} & \text{if } i=j \\ E_{ii}+E_{jj}-E_{ij}-E_{ji} & \text{if } i \neq j, \end{cases}$$

where E_{ij} is the $n \times n$ matrix with 1 in its ijth position and 0's elsewhere.

The basis functions, which have been used in our calculation have the form

$$|\varphi_k\rangle = |r_1^{2m_k}e^{-\mathbf{r}'\bar{A}_k\mathbf{r}}\rangle = |r_1^{2m_k}\phi_k\rangle, \qquad (A4)$$

where $\bar{A}_k$ is a symmetric and positive definite matrix of nonlinear variational parameters. The notation $\bar{A}_k$ denotes a Kronecker product of the A_k matrix with the 3×3 identity matrix, I_3. Any integral with even power of interparticle distance r_{st}^{2n} can be calculated using following expression:

$$r_{st}^{2n} = [\mathbf{r}'(J_{st} \otimes I_3)\mathbf{r}]^n = (-1)^n \left.\frac{\partial^n e^{-\alpha\mathbf{r}'\bar{J}_{st}\mathbf{r}}}{\partial\alpha^n}\right|_{\alpha=0}. \qquad (A5)$$

In particular, if $s \equiv t=1$, r_1^{2n} can be generated as

$$r_1^{2n} \equiv r_{11}^{2n} = (-1)^n \left.\frac{\partial^n e^{-\alpha\mathbf{r}'\bar{J}_{11}\mathbf{r}}}{\partial\alpha^n}\right|_{\alpha=0}.$$

Any integrals with odd power of premultipliers r_{st}^{2n-1} can be found by using the following integral representation of r_{st}^{-1}:

$$r_{st}^{-1} = \frac{2}{\sqrt{\pi}}\int_0^{\infty} dx\ e^{-x^2\mathbf{r}'\bar{J}_{st}\mathbf{r}}. \qquad (A6)$$

The expression for the overlap integral of basis functions (A4) is well known and has the following form:[12]

$$\langle\varphi_k|\varphi_l\rangle = \langle\phi_k|\phi_l\rangle(3/2)_{m_k+m_l}(\text{Tr}[J_{11}A_{kl}^{-1}])^{m_k+m_l}, \qquad (A7)$$

where $\langle\phi_k|\phi_l\rangle = \Gamma[1/2]|A_{kl}|^{-3/2}$ is the elemental overlap integral, and A_{kl}^{-1} is the inverse matrix. Vertical bars applied to a matrix denote the determinant of the matrix.

In order to evaluate the structural integrals, we combine some useful matrix properties into two theorems. Theorem A.1 can be found in Ref. 22 and Theorem A.2 has been taken from Ref. 23.

Theorem A.1. Let A and B be $n \times n$ matrices. Then

$$|A \otimes B| = |A|^n|B|^n,$$

$$\text{Tr}[A+B] = \text{Tr}[A] + \text{Tr}[B].$$

Theorem A.2. Let G and $G+H$ be nonsingular matrices with $H=\Sigma_{i=1}^N H_i$, $C_1=G$, $C_{i+1}^{-1}=C_i^{-1}-\nu_i C_i^{-1}H_iC_i^{-1}$, $\nu_i^{-1}=1+\text{Tr}[C_i^{-1}H_i]$ and let H_i be matrix of rank 1. Then

$$|G+H| = |G|\prod_{i=1}^N \nu_i^{-1}.$$

Taking into account that any premulitplier in the structural integrals can be expressed in the exponential form [Eqs. (A5) and (A6)], and using Theorem A.1 and Theorem A.2, the structural integral in the general form for even and odd powers $(R_e = \langle\varphi_k|r_{ij}^{2N}|\varphi_l\rangle, R_o = \langle\varphi_k|r_{ij}^{2N-1}|\varphi_l\rangle)$ can be reduced to a product of derivatives of the elemental overlap integral:

$$
\begin{aligned}
R_o &= \langle\varphi_k|r_{ij}^{2N-1}|\varphi_l\rangle = \langle e^{-\mathbf{r}'\bar{A}_k\mathbf{r}}|r_1^{\overbrace{2(m_k+m_l)}^{M}}r_{ij}^{2N}r_{ij}^{-1}|e^{-\mathbf{r}'\bar{A}_l\mathbf{r}}\rangle = \langle\phi_k|r_1^{2M}r_{ij}^{2N}r_{ij}^{-1}|\phi_l\rangle \\
&= (-1)^{M+N}\frac{\partial^M}{\partial\alpha^M}\frac{\partial^N}{\partial\beta^N}\langle\phi_k|\frac{2}{\sqrt{\pi}}\int_0^{\infty} dx\ e^{-\mathbf{r}'(\alpha\bar{J}_{11}+\beta\bar{J}_{ij}+x^2\bar{J}_{ij})\mathbf{r}}|\phi_l\rangle\Big|_{\alpha=\beta=0} \\
&= (-1)^{M+N}\frac{2}{\sqrt{\pi}}\frac{\partial^M}{\partial\alpha^M}\frac{\partial^N}{\partial\beta^N}\int_0^{\infty} dx\int_{-\infty}^{\infty} dr\ e^{-\mathbf{r}'(\bar{A}_{kl}+\alpha\bar{J}_{11}+(x^2+\beta)\bar{J}_{ij})\mathbf{r}}\Big|_{\alpha=\beta=0} \\
&= (-1)^{M+N}\frac{2}{\sqrt{\pi}}\frac{\partial^M}{\partial\alpha^M}\frac{\partial^N}{\partial\beta^N}\pi^{3n/2}\int_0^{\infty} dx|\bar{A}_{kl}+\alpha\bar{J}_{11}+(x^2+\beta)\bar{J}_{ij}|^{-1/2}\Big|_{\alpha=\beta=0} \\
&= (-1)^{M+N}\frac{2}{\sqrt{\pi}}\frac{\partial^M}{\partial\alpha^M}\frac{\partial^N}{\partial\beta^N}\int_0^{\infty} dx\ \pi^{3n/2}|A_{kl}|^{-3/2}|I_n+\alpha J_{11}A_{kl}^{-1}+(x^2+\beta)J_{ij}A_{kl}^{-1}|^{-3/2}\Big|_{\alpha=\beta=0}
\end{aligned}
$$

$$
\begin{aligned}
&= (-1)^{M+N}\frac{2}{\sqrt{\pi}}\langle\phi_k|\phi_l\rangle\frac{\partial^M}{\partial\alpha^M}\frac{\partial^N}{\partial\beta^N}\int_0^\infty dx\,|I_n + \alpha\overbrace{J_{11}A_{kl}^{-1}}^{H_1} + (x^2+\beta)\overbrace{J_{ij}A_{kl}^{-1}}^{H_2}|^{-3/2}\bigg|_{\alpha=\beta=0}\\[2mm]
&= (-1)^{M+N}\langle\phi_k|\phi_l\rangle\frac{2}{\sqrt{\pi}}\frac{\partial^M}{\partial\alpha^M}\frac{\partial^N}{\partial\beta^N}\int_0^\infty dx\,|I_n + \alpha H_1 + (x^2+\beta)H_2|^{-3/2}\bigg|_{\alpha=\beta=0}\\[2mm]
&= (-1)^{M+N}\langle\phi_k|\phi_l\rangle\frac{2}{\sqrt{\pi}}\frac{\partial^M}{\partial\alpha^M}\frac{\partial^N}{\partial\beta^N}\int_0^\infty dx\,[\nu_1^{-1}(\alpha)\nu_2^{-1}(x^2,\beta,\alpha)]^{-3/2}\bigg|_{\alpha=\beta=0}\\[2mm]
&= (-1)^{M+N}\langle\phi_k|\phi_l\rangle\frac{2}{\sqrt{\pi}}\frac{\partial^M}{\partial\alpha^M}[\nu_1^{-1}(\alpha)]^{-3/2}\frac{\partial^N}{\partial\beta^N}\int_0^\infty dx\,[\nu_2^{-1}(x^2,\beta,\alpha)]^{-3/2}\bigg|_{\alpha=\beta=0},
\end{aligned}
\tag{A8}
$$

where ν_1 and ν_2 are defined in Theorem A.2.

Integrating and differentiating the last term in (A8) with respect to β we obtain

$$
\begin{aligned}
\eta &= (-1)^N\frac{\partial^N}{\partial\beta^N}\int_0^\infty dx\,\nu_2^{3/2} = (-1)^N\frac{\partial^N}{\partial\beta^N}\int_0^\infty dx\{1+(x^2+\beta)\mathrm{Tr}[C_2^{-1}H_2]\}^{-3/2} = (-1)^N\frac{\partial^N}{\partial\beta^N}(\mathrm{Tr}[C_2^{-1}H_2])^{-1/2}(1+\beta\,\mathrm{Tr}[C_2^{-1}H_2])^{-1}\\[2mm]
&= N!\,(\mathrm{Tr}[C_2^{-1}H_2])^{-1/2}(\mathrm{Tr}[C_2^{-1}H_2])^N(1+\beta\,\mathrm{Tr}[C_2^{-1}H_2])^{-(N+1)}.
\end{aligned}
$$

Then, setting $\beta=0$, expanding C_2^{-1}, taking into account that $C_1=I_n$, and using Taylor expansion (A1) yields the following:

$$
\eta_{\beta=0} = N!\,(\mathrm{Tr}[C_2^{-1}H_2])^{N-1/2} = N!\,(\mathrm{Tr}[H_2] - \nu_1\alpha\,\mathrm{Tr}[H_1H_2])^{N-1/2} = N!\,(\mathrm{Tr}[H_2])^{N-1/2}\sum_{k=0}^\infty\frac{(N-k+1/2)_k}{k!}\left(-\nu_1\alpha\frac{\mathrm{Tr}[H_1H_2]}{\mathrm{Tr}[H_2]}\right)^k.
\tag{A9}
$$

Now, differentiating of $\nu_1^{k+3/2}\alpha^k$ with respect to α and recalling the Leibniz formula (A2) we obtain

$$
\begin{aligned}
\zeta &= \frac{\partial^M\nu_1^{k+3/2}\alpha^k}{\partial\alpha^M}\bigg|_{\alpha=0} = \sum_{m=0}^M\binom{M}{m}\frac{\partial^m\alpha^k}{\partial\alpha^m}\frac{\partial^{M-m}\nu_1^{k+3/2}}{\partial\alpha^{M-m}}\bigg|_{\alpha=0} = \sum_{m=0}^M\binom{M}{m}\frac{k!\,\alpha^{k-m}}{(k-m)!}\frac{\partial^{M-m}(1+\alpha\,\mathrm{Tr}[H_1])^{-(k+3/2)}}{\partial\alpha^{M-m}}\bigg|_{\alpha=0}\\[2mm]
&= \sum_{m=0}^M\binom{M}{m}\frac{k!\,\alpha^{k-m}}{(k-m)!}\,(-1)^{M-m}\left(k+\frac{3}{2}\right)_{M-m}(\mathrm{Tr}[H_1])^{M-m}(1+\alpha\,\mathrm{Tr}[H_1])^{-(k+3/2+M-m)}\bigg|_{\alpha=0}\\[2mm]
&= \sum_{m=0}^M\binom{M}{m}\frac{k!\,\delta_{km}}{(k-m)!}(-1)^{M-m}\left(k+\frac{3}{2}\right)_{M-m}(\mathrm{Tr}[H_1])^{M-m} = (-1)^{M-k}\frac{M!}{(M-k)!}\frac{\Gamma\left[M+\dfrac{3}{2}\right]}{\Gamma\left[k+\dfrac{3}{2}\right]}(\mathrm{Tr}[H_1])^{M-k}.
\end{aligned}
\tag{A10}
$$

Next, multiplying Eq. (A9) by $\nu_1^{3/2}$, differentiating with respect to α, and applying (A10) gives

$$
\begin{aligned}
\xi_{\alpha=0} &= (-1)^M\frac{\partial^M\nu_1^{3/2}\,\eta|_{\beta=0}}{\partial\alpha^M}\bigg|_{\alpha=0} = (-1)^M N!\,(\mathrm{Tr}[H_2])^{N-1/2}\sum_{k=0}^\infty\frac{(N-k+1/2)_k}{k!}\left(-\frac{\mathrm{Tr}[H_1H_2]}{\mathrm{Tr}[H_2]}\right)^k\frac{\partial^M\nu_1^{k+3/2}\alpha^k}{\partial\alpha^M}\bigg|_{\alpha=0}\\[2mm]
&= N!\,(\mathrm{Tr}[H_1])^M(\mathrm{Tr}[H_2])^{N-1/2}\sum_{k=0}^{\min(M,\infty)}\frac{(N-k+1/2)_k M!}{(M-k)!\,k!}\frac{\Gamma\left[M+\dfrac{3}{2}\right]}{\Gamma\left[k+\dfrac{3}{2}\right]}\left(\frac{\mathrm{Tr}[H_1H_2]}{\mathrm{Tr}[H_1]\mathrm{Tr}[H_2]}\right)^k.
\end{aligned}
\tag{A11}
$$

Finally, substituting Eq. (A11) into Eq. (A8) we find structural integral for odd power of r_{ij}:

$$R_o = \frac{2}{\sqrt{\pi}} \langle \phi_k | \phi_l \rangle \Gamma\left[M + \frac{3}{2}\right] (\mathrm{Tr}[H_1])^M N! \, (\mathrm{Tr}[H_2])^{N-1/2} \sum_{k=0}^{M} \binom{M}{k} \frac{\Gamma\left[N + \frac{1}{2}\right]}{\Gamma\left[N - k + \frac{1}{2}\right] \Gamma\left[k + \frac{3}{2}\right]} \left(\frac{\mathrm{Tr}[H_1 H_2]}{\mathrm{Tr}[H_1]\mathrm{Tr}[H_2]}\right)^k$$

$$= \langle \varphi_k | \varphi_l \rangle N! \, (\mathrm{Tr}[H_2])^{N-1/2} \sum_{k=0}^{M} \binom{M}{k} \frac{\Gamma\left[N + \frac{1}{2}\right]}{\Gamma\left[N - k + \frac{1}{2}\right] \Gamma\left[k + \frac{3}{2}\right]} \left(\frac{\mathrm{Tr}[H_1 H_2]}{\mathrm{Tr}[H_1]\mathrm{Tr}[H_2]}\right)^k$$

$$= \langle \varphi_k | \varphi_l \rangle (\mathrm{Tr}[H_2])^{N-1/2} \frac{1}{\Gamma[3/2]} N! \, _2F_1\left[\frac{1}{2} - N, -M, \frac{3}{2}, \frac{\mathrm{Tr}[H_1 H_2]}{\mathrm{Tr}[H_1]\mathrm{Tr}[H_2]}\right], \tag{A12}$$

where $_2F_1(a,b,c,x)$ is the hypergeometric function.

If we remove r_{ij}^{-1} from Eq. (A8) then we can get the formula for the structural integral with even powers in the following form:

$$R_e = (-1)^{M+N} \langle \phi_k | \phi_l \rangle \frac{\partial^M}{\partial \beta^M} [\nu_1^{-1}(\alpha)]^{-3/2}$$

$$\times \frac{\partial^N}{\partial \alpha^N} [\nu_2^{-1}(\beta,\alpha)]^{-3/2} \Bigg|_{\alpha=\beta=0}. \tag{A13}$$

Applying the definition of ν_2 from Theorem A.2, for the last term in Eq. (A13) we obtain

$$\eta = (-1)^N \left. \frac{\partial^N (\nu_2^{-1})^{-3/2}}{\partial \beta^N} \right|_{\beta=0}$$

$$= (-1)^N \left. \frac{\partial (1 + \beta \, \mathrm{Tr}[C_2^{-1} H_2])^{-3/2}}{\partial \beta^N} \right|_{\beta=0}$$

$$= \left(\frac{3}{2}\right)_N (\mathrm{Tr}[C_2^{-1} H_2])^N (\nu_2^{-1})^{-(N+3/2)} \Bigg|_{\beta=0}$$

$$= \left(\frac{3}{2}\right)_N (\mathrm{Tr}[C_2^{-1} H_2])^N. \tag{A14}$$

Now, multiplying η by the $\nu^{3/2}$, setting $C_1 = I_n$, expanding ν_1, results the following expression after simplification:

$$\zeta = \nu_1^{3/2} \eta |_{\beta=0} = \nu_1^{3/2} \left(\frac{3}{2}\right)_N (\mathrm{Tr}[C_2^{-1} H_2])^N$$

$$= \left(\frac{3}{2}\right)_N \nu_1^{3/2} (\mathrm{Tr}[C_1^{-1} H_2] - \nu_1 \alpha \, \mathrm{Tr}[C_1^{-1} H_1 C_1^{-1} H_2])^N$$

$$= \left(\frac{3}{2}\right)_N \nu_1^{3/2} (\mathrm{Tr}[H_2] - \nu_1 \alpha \, \mathrm{Tr}[H_1 H_2])^N = \left(\frac{3}{2}\right)_N \sum_{k=0}^{N} \binom{N}{k}$$

$$\times (\mathrm{Tr}[H_2])^{N-k} (-\mathrm{Tr}[H_1 H_2])^k \alpha^k \nu_1^{k+3/2}$$

$$= \left(\frac{3}{2}\right)_N (\mathrm{Tr}[H_2])^N \sum_{k=0}^{N} \binom{N}{k} \left(\frac{-\mathrm{Tr}[H_1 H_2]}{\mathrm{Tr}[H_2]}\right)^k$$

$$\times \alpha^k (1 + \alpha \, \mathrm{Tr}[H_1])^{-(k+3/2)}. \tag{A15}$$

Differentiating ζ with respect to α and recalling the Leibniz formula (A3) we have

$$\xi_{\alpha=0} = (-1)^M \frac{\partial^M \zeta}{\partial \alpha^M}\Bigg|_{\alpha=0} = (-1)^M \left(\frac{3}{2}\right)_N (\mathrm{Tr}[H_2])^N \sum_{k=0}^{N} \binom{N}{k}$$

$$\times \left(\frac{-\mathrm{Tr}[H_1 H_2]}{\mathrm{Tr}[H_2]}\right)^k \sum_{m=0}^{M} \binom{M}{m} \frac{\partial^m \alpha^k}{\partial \alpha^m} \frac{\partial^{M-m}}{\partial \alpha^{M-m}}$$

$$\times (1 + \alpha \, \mathrm{Tr}[H_1])^{-(k+3/2)} \Bigg|_{\alpha=0}$$

$$= (-1)^M \left(\frac{3}{2}\right)_N (\mathrm{Tr}[H_2])^N \sum_{k=0}^{N} \binom{N}{k} \left(\frac{-\mathrm{Tr}[H_1 H_2]}{\mathrm{Tr}[H_2]}\right)^k \sum_{m=0}^{M} \binom{M}{m}$$

$$\times \frac{k! \, \alpha^{k-m}}{(k-m)!} (-1)^{M-m} \left(k + \frac{3}{2}\right)_{M-m} (\mathrm{Tr}[H_1])^{M-m}$$

$$\times (1 + \alpha \, \mathrm{Tr}[H_1])^{-(k+3/2+M-m)} \Bigg|_{\alpha=0}$$

$$= \left(\frac{3}{2}\right)_N (\mathrm{Tr}[H_1])^M (\mathrm{Tr}[H_2])^N \sum_{k=0}^{N} \binom{N}{k}$$

$$\times \left(\frac{-\mathrm{Tr}[H_1 H_2]}{\mathrm{Tr}[H_2]}\right)^k \sum_{m=0}^{M} \binom{M}{m} \frac{k!}{(k-m)!} \left(k + \frac{3}{2}\right)_{M-m}$$

$$\times (-\mathrm{Tr}[H_1])^{-m} \delta_{km} = \left(\frac{3}{2}\right)_N (\mathrm{Tr}[H_1])^M \Gamma\left[M + \frac{3}{2}\right]$$

$$\times (\mathrm{Tr}[H_2])^N \sum_{k=0}^{\min(N,M)}$$

$$\times \binom{N}{k} \frac{M!}{(M-k)! \, \Gamma\left[k + \frac{3}{2}\right]} \left(\frac{\mathrm{Tr}[H_1 H_2]}{\mathrm{Tr}[H_1]\mathrm{Tr}[H_2]}\right)^k. \tag{A16}$$

Finally, after substituting Eq. (A16) into Eq. (A13), the structural integral for even power of r_{ij} is given by

$$R_e = \langle \phi_k | \phi_l \rangle \left(\frac{3}{2} \right)_N (\mathrm{Tr}[H_1])^M \Gamma \left[M + \frac{3}{2} \right] (\mathrm{Tr}[H_2])^N$$

$$\times \sum_{k=0}^{\min(N,M)} \binom{N}{k} \frac{M!}{(M-k)! \, \Gamma\left[k + \frac{3}{2}\right]} \left(\frac{\mathrm{Tr}[H_1 H_2]}{\mathrm{Tr}[H_1]\mathrm{Tr}[H_2]} \right)^k$$

$$(A17)$$

$$= \langle \varphi_k | \varphi_l \rangle \Gamma \left[N + \frac{3}{2} \right] (\mathrm{Tr}[H_2])^N \sum_{k=0}^{\min(N,M)}$$

$$\times \binom{N}{k} \frac{M!}{(M-k)! \, \Gamma\left[k + \frac{3}{2}\right]} \left(\frac{\mathrm{Tr}[H_1 H_2]}{\mathrm{Tr}[H_1]\mathrm{Tr}[H_2]} \right)^k .$$

Expressions (A12) and (A17) will apply to r_1 and r_2, if we set $i \equiv j$ and $i = 1, 2$.

For $N = 1$, the structural integrals [Eqs. (A12) and (A17)] have the following simple form:

$$R_o = \langle \varphi_k | \varphi_l \rangle (\mathrm{Tr}[H_2])^{1/2} \frac{{}_2F_1\left[-\frac{1}{2}, -M, \frac{3}{2}, \frac{\mathrm{Tr}[H_1 H_2]}{\mathrm{Tr}[H_1]\mathrm{Tr}[H_2]} \right]}{\Gamma\left[\frac{3}{2}\right]},$$

$$R_e = \langle \varphi_k | \varphi_\ell \rangle \mathrm{Tr}[H_2] \left(\frac{3}{2} + M \frac{\mathrm{Tr}[H_1 H_2]}{\mathrm{Tr}[H_2]\mathrm{Tr}[H_1]} \right). \qquad (A18)$$

[1] A. Carrington, I. R. McNab, and C. A. Montgomerie, J. Phys. B **22**, 3551 (1989).

[2] I. Ben-Itzhak, E. Wells, K. D. Carnes, V. Krishnamurthi, O. L. Weaver, and B. D. Esry, Phys. Rev. Lett. **85**, 58 (2000).

[3] A. Carrington, I. R. McNab, C. A. Montgomerie-Leach, and R. A. Kennedy, Mol. Phys. **72**, 735 (1991).

[4] R. E. Moss and I. A. Sadler, Mol. Phys. **61**, 905 (1987).

[5] B. D. Esry and H. R. Sadeghpour, Phys. Rev. A **60**, 3604 (1999).

[6] R. E. Moss and L. Valenzano, Mol. Phys. **100**, 649 (2002).

[7] S. Bubin, E. Bednarz, and L. Adamowicz, J. Chem. Phys. **122**, 041102 (2005).

[8] D. M. Bishop, Phys. Rev. Lett. **37**, 484 (1976).

[9] D. M. Bishop and L. M. Cheung, Phys. Rev. A **16**, 640 (1977).

[10] A. M. Frolov, Phys. Rev. A **67**, 064501 (2003).

[11] M. Cafiero, S. Bubin, and L. Adamowicz, Phys. Chem. Chem. Phys. **5**, 1491 (2003).

[12] D. B. Kinghorn and L. Adamowicz, J. Chem. Phys. **110**, 7166 (1999).

[13] D. B. Kinghorn and L. Adamowicz, Phys. Rev. Lett. **83**, 2541 (1999).

[14] C. E. Scheu, D. B. Kinghorn, and L. Adamowicz, J. Chem. Phys. **114**, 3393 (2001).

[15] S. Bubin and L. Adamowicz, J. Chem. Phys. **118**, 3079 (2003).

[16] S. Bubin and L. Adamowicz, J. Chem. Phys. **120**, 6051 (2004).

[17] S. Bubin and L. Adamowicz, J. Chem. Phys. **121**, 6249 (2004).

[18] H. J. Monkhorst, Int. J. Quantum Chem. **72**, 281 (1999).

[19] M. Cafiero and L. Adamowicz, Chem. Phys. Lett. **387**, 136 (2004).

[20] See CODATA 2002 recommended values and NIST Physical Reference Data at http://physics.nist.gov/

[21] S. Bubin and L. Adamowicz, Chem. Phys. Lett. **403**, 185 (2005).

[22] D. B. Kinghorn, Int. J. Quantum Chem. **57**, 141 (1996).

[23] K. S. Miller, *Some Eclectic Matrix Theory* (Robert E. Kriger, Malabar, FL, 1987).